THE JOURNAL OF BIOLOGICAL CHEMISTRY
Vol. 277, No. 34, Issue of August 23, pp. 30984–30990, 2002
Printed in U.S.A.
© 2002 by The American Society for Biochemistry and Molecular Biology, Inc.

Unusual Mode of Binding of Human Group IIA Secreted Phospholipase A_2 to Anionic Interfaces as Studied by Continuous Wave and Time Domain Electron Paramagnetic Resonance Spectroscopy*

Received for publication, April 15, 2002, and in revised form, May 30, 2002
Published, JBC Papers in Press, May 30, 2002, DOI 10.1074/jbc.M203649200

Stéphane Canaan‡§¶, Robert Nielsen‡¶, Farideh Ghomashchi‡§, Bruce H. Robinson‡‖, and Michael H. Gelb‡§‖

From the Departments of ‡Chemistry and §Biochemistry, University of Washington, Seattle, Washington 98195

Human group IIA phospholipase A_2 (hGIIA) is secreted from a number of cells during inflammation and is known to interact strongly with anionic membranes and to exhibit potent Gram-positive bactericidal activity. This protein contains 23 cationic residues, which are scattered over its entire surface, resulting in a high pI of 9.39. To understand the molecular basis for the selective binding of hGIIA to anionic membranes, 14 single-site, spin-labeled hGIIA proteins were analyzed in the presence and absence of vesicles of anionic phospholipid by time domain and continuous wave electron paramagnetic resonance (EPR) spin relaxant techniques. Surprisingly, for hGIIA bound to anionic vesicles, all of the spin labels were highly protected from water-soluble spin relaxants. Together with light scattering studies, these EPR results suggest the formation of a supramolecular aggregate involving clusters of hGIIA molecules bridging together multiple vesicles. This anomalous mode of binding of hGIIA to anionic phospholipid explains previous data in which charge reversal mutation of a few cationic residues on multiple faces of hGIIA leads to a comparable and modest reduction in affinity of the protein for anionic vesicles. In the presence of mixed micelles composed of 10% anionic phospholipids in Triton X-100 a monodisperse protein-lipid complex is formed. Under these conditions, the EPR methods were used to map the surface of hGIIA that constitutes the interfacial binding site (IBS). The IBS of hGIIA consists of the highly hydrophobic surface that surrounds the opening to the active site slot.

The secreted phospholipases A_2 ($sPLA_2$s)[1] are water-soluble proteins that must bind to the membrane-water interface to access their substrates. Catalysis consists of: adsorption and possible penetration of the enzyme into the membrane and binding of a single phospholipid molecule in the active site (1). The molecular basis for preferential binding to membranes of different phospholipid composition is only partly understood (1–5). A key issue in understanding the behavior of $sPLA_2$s is to determine why different members of this family of enzymes display dramatically different affinities for membranes composed of anionic *versus* zwitterionic phospholipids. For example, human group X $sPLA_2$ displays high enzymatic activity on both anionic phosphatidylserine and zwitterionic phosphatidylcholine vesicles, whereas human group IIA $sPLA_2$ (hGIIA) hydrolyzes anionic vesicles several orders of magnitude faster than zwitterionic vesicles (6, 7). Differential interfacial binding to anionic *versus* zwitterionic membranes accounts for the differences in kinetic behavior of these two $sPLA_2$s, rather than the differences in the abilities of the active sites to accomodate phospholipids with different polar head groups.[2] This has direct physiological consequences. For example, hGIIA readily acts on the highly anionic phosphatidylglycerol-rich outer membrane of a variety of Gram-positive bacteria (8–10) and is the principal Gram-positive bactericidal agent in human tears (11). This enzyme does not act on the corneal endothelial cells, because it cannot bind to the phosphatidylcholine-rich outer plasma membrane of these cells (12). In some cells that have been transfected with hGIIA, this $sPLA_2$ acts on membranes to release arachidonic acid for eicosanoid biosynthesis. The enzyme, in this case, however, does not act on the external face of the plasma membrane, but rather may be acting in specialized intracellular membrane compartments (13).

A new technique using electron paramagnetic resonance (EPR) spectroscopy has been recently developed to study the binding of peripheral membrane proteins to the interface of anionic phospholipid vesicles (14, 15). This method involves site-specific labeling of the protein with a nitroxide and the use of an aqueous- or membrane-soluble spin relaxant to measure the distance of the spin label from the membrane-aqueous interface. Studies using this method have shown that interfacial binding of bee venom $sPLA_2$ is driven by the shallow penetration into the membrane of a collar of hydrophobic res-

* This work was supported by Grants HL36235, HL50040, and GM065944 from the National Institutes of Health. The Bruker EMX EPR spectrometer used for some CW measurements was funded under the UW Environmental Sciences Center Grant P30-ESO7033 from the NIEHS. The costs of publication of this article were defrayed in part by the payment of page charges. This article must therefore be hereby marked "*advertisement*" in accordance with 18 U.S.C. Section 1734 solely to indicate this fact.

¶ These authors contributed equally to this work.

‖ To whom correspondence and reprint requests may be addressed: Depts. of Chemistry and Biochemistry, Box 351700, University of Washington, Seattle, WA 98195. E-mail: gelb@chem.washington.edu and robinson@chem.washington.edu.

[1] The abbreviations used are: $sPLA_2$, secreted phospholipase A_2; hGIIA, human group IIA secreted phospholipase A_2; IBS, interfacial binding site; LUV, large unilamellar vesicles; TD, time domain; CW, continuous wave; DTT, dithiothreitol; Crox, tris(oxalato)chromate(III); NiEDDA, nickel(ethylenediaminediacetic acid); DOPM, 1,2-dioleoylphosphatidylmethanol; DTPM, 1,2-ditetradecylphosphatidylmethanol; $DO_{et}PC$, 1,2-di-*O*-octadecenylphosphatidylcholine; $DO_{et}PS$, 1,2-di-*O*-octadecenylphosphatidylserine; SR, saturation recovery; pELDOR, pulsed electron double resonance; CTPO, 3-carboxy-2,2,5,5-tetramethylpyrrolidinyloxyl. Spin label mutants are designated S120C-sl for serine-120 replaced by spin-labeled cysteine, for example.

[2] S. Bezzine, J. Bollinger, S. L. Veatch, S. L. Keller, and M. H. Gelb, submitted for publication.

This paper is available on line at http://www.jbc.org

idues that surround the opening to the active site slot (14). Other studies have shown that the C2 domain of cytosolic phospholipase A_2 penetrates into the hydrophobic interior of the membrane below the phospholipid head group region using two hydrophobic residue-rich surface loops (15). The EPR method provides an accurate orientation of the protein with respect to the membrane surface.

In the current study, we have applied this EPR method to study the structural features of binding of hGIIA to anionic phospholipid vesicle membranes and to mixed micelles of anionic phospholipid dispersed in Triton X-100 aggregates. In addition, we report the first example of the use of time domain (TD) EPR techniques for protein-membrane docking, which complements the continuous wave (CW) method used previously (14, 15). Our results reveal a number of unusual features governing the binding of highly basic hGIIA (pI of 9.39, due to the presence of 13 lysines and 10 arginines scattered over the surface of the protein) to anionic phospholipid surfaces. These features help to explain the dramatic dependence of the interfacial binding of hGIIA on the presence of anionic phospholipids in the lipid aggregate.

MATERIALS AND METHODS

Preparation of Spin-labeled hGIIA Proteins—Expression of hGIIA in *Escherichia coli*, site-directed mutagenesis, refolding hGIIA from inclusion bodies, and protein refolding and purification were carried out as described (12). Each mutant at 1.6–2 mg/ml (OD_{280} using $\epsilon^{1\%} = 9$ (12)) was incubated in 50 mM Tris, pH 8.0, 1 mM DTT on ice for 30 min followed by addition of 1.5 mM spin label reagent ((1-oxyl-2,2,5,5-tetramethyl-3 pyrroline-3-methyl)methanethiosulfonate, Toronto Research Chemicals, Toronto, Ontario, Canada). After 50 min, the sample was passed twice through a column of 1 ml Sephadex G-25. The eluant was concentrated to 3.5–4 mg/ml protein in a Microcon 10 (Millipore). Mutants containing the charge reversal cluster (K52E/R53E/K56E/R57E) were reduced with 0.1 mM DTT on ice for 30 min, because higher thiol concentrations led to a decrease in enzymatic activity. DTT was removed by buffer addition and concentration using a Microcon 10. This was repeated three times, and finally spin labeling reagent was added to 0.5 mM, and the sample was processed as above. All spin-labeled proteins were >98% pure (SDS-PAGE), and specific activities were 65–100% of the wild type value (fluorimetric assay (16)). Specific activities on mixed micelles (Table I) were measured with 2.5 mM Triton X-100, 1 mM NaCl, 0.6 mM $CaCl_2$, 250 μM 1,2-dioleoylphosphatidylmethanol (DOPM) (Avanti) at pH 8.0 and 25 °C using a pH-stat (17).

Preparation of EPR Samples—Large unilamellar vesicles (LUV) of 1,2-ditetradecylphosphatidylmethanol (DTPM) were prepared by extrusion of 50 mM lipid in EPR buffer (50 mM Tris-HCl, pH 8.0, 0.5 mM $CaCl_2$) using a Mini-Extruder (Avanti) (first through two 0.8-μm membranes, Nuclepore, followed by a second pass through two 0.1-μm membranes; lipid concentration determined by phosphate assay). The size of vesicles was confirmed to be 0.105 μm with a polydispersity of 0.089 using a BIC Particle Analyzer (Brookhaven Instruments). EPR samples contained 42–50 μM hGIIA with or without 25 mM DTPM in EPR buffer with or without 10 mM tris(oxalato)chromate(III) (Crox) or 10 mM nickel(ethylenediaminediacetic acid) (NiEDDA) (18, 19) in a Teflon capillary tube (24 LW, Zeus) sealed with wax (Cristoseal). Nitrogen (99%) or oxygen (medical air) was passed through the EPR sample chamber at 21 °C to saturate the sample with the desired gas (by diffusion through the sample tube in <20 min). Samples with mixed micelles contained 12.6 mM DTPM and 126 mM Triton X-100 instead of LUV. Some experiments were carried out with co-vesicles of DTPM or $DO_{et}PS$ in $DO_{et}PC$ (20).

EPR Experiments—EPR spectra were acquired with a loop-gap resonator (21). TD experiments were used to measure the electron spin-lattice relaxation rate ($R_1 = 1/T_1$), where T_1 is the electron spin-lattice relaxation time. These TD experiments included saturation recovery (SR) and pulsed electron double resonance (pELDOR) EPR spectroscopies (21–23). pELDOR measurements were primarily limited to solution conditions with and without oxygen because of signal to noise at the ~45 μM protein concentrations used. CW data were collected on all protein samples with and without LUV using the power saturation method to measure the rollover parameter P_2 (14, 15). The S120C-sl electrostatic potential was measured using SR and pELDOR methods (14, 15, 24, 25). The ^{15}N relaxants used were 1 mM TEMPAMINE (2,2,6,6-tetramethylpiperidine-1-oxyl-4-amine) or 1 mM TEMPOL (2,2,6,6-tetramethylpiperidine-1-oxyl-4-ol) or 1 mM CTPO (3-carboxy-2,2,5,5-tetramethylpyrrolidinyloxyl), labeled at N_1 with ^{15}N (gift from Dr. A. H. Beth, Vanderbilt University).

Light Scattering—Right angle scattering was measured in a spectrofluorometer (ex/em 500 nm, 6 nm slits) on samples containing 1 ml of EPR buffer with 50 μM DTPM vesicles and 85 nM hGIIA at 22 °C.

Electrostatics—An electrostatic calculation was carried out to explore the stability of the protein-vesicle supramolecular aggregate described under "Discussion." The calculation was done on a subset of the supramolecular structure, comprising two LUV, each of radius 500 Å, brought into proximity by a patch of protein on the surface of one of the LUV. The patch was modeled as a planar disc with a uniform charge density given by the difference in charge between the proteins and the lipid beneath. In the model, each protein contains 20 positive charges, and the protein density within the disc is given in the discussion section. Each lipid contains a single negative charge and occupies 70 Å^2. The electrostatic potential of this system was calculated for a grided surface over the LUV and the patch assuming a screened coulomb interaction. The calculation was carried out as a function of the distance between the patch (on one LUV) and the second LUV. The system is attractive when the characteristic screening length is less than 55 Å. The ionic strength of the buffer predicts a Debye screening length of around 15 Å for the EPR buffer; therefore we are well within the range of attraction.

RESULTS

Preparation of Spin-labeled hGIIA Mutants—Twelve single-site hGIIA mutant proteins were produced by replacing a surface residue with cysteine and tagging its SH group with a nitroxyl reagent (14, 15). Mutated residues were chosen from the x-ray structure (26) to provide coverage of the entire surface of hGIIA. Residues 3, 10, and 19 are on the putative interfacial binding surface (IBS) previously proposed (12, 27, 28), residues 23, 63, and 70 are near the proposed IBS, and residues 35, 56, 104, 113, 115, and 120 are away from the proposed IBS. The specific activities for the mutants on DOPM/Triton X-100 mixed micelles are all similar (Table I). Two spin-labeled mutants were also prepared (nitroxide at positions 56 and 120) containing the charge reversal mutation cluster K52E/R53E/K56E/R57E. Although the respective specific activities of 70 and 92% of wild type suggest a native structure, these proteins were more sensitive than the others to DTT-induced reduction of hGIIA disulfides, suggesting a lower stability.

CW and TD EPR Data from Spin-labeled hGIIA on DTPM LUV—Site-specific nitroxide-labeled proteins are used as a basis for locating the position of each spin label relative to a membrane interface. The interface, which is composed of negatively charged lipids, generates an electrostatic gradient. This electrostatic gradient creates a concentration gradient of Crox, because Crox is a water-soluble, membrane-impenetrable, negatively charged spin relaxant (14, 15). Exposure of the nitroxide within the Crox gradient is defined by four experimental conditions: protein in the presence and absence of vesicles and in the presence and absence of Crox. The shift ($\Delta P_2 = P_2^{+Crox} - P_2^{-Crox}$ of the CW EPR rollover parameter P_2 upon addition of Crox measures the collision-induced relaxation of nitroxide, which is proportional to the local concentration of Crox (14, 21). Measurements in the absence of membrane account for the effect of the local protein electrostatic potential on the concentration of Crox and provide a reference for the response to Crox for each spin-labeled mutant. From previous studies on proteins with values of pI near neutrality, a bulk concentration of 10 mM Crox was found to give a response which made optimal use of the finite range of the experimentally obtainable P_2 values. In each case, the local electrostatic effect of the protein was weak, and membrane electrostatics dominated the distribution of Crox in the vicinity of the protein when bound to the membrane surface (14, 15).

TABLE I

Relaxation data for hGIIA on LUV of DTPM with Crox and on mixed-micelles (10% DTPM/Triton X-100) with Crox and NiEDDA

Relaxation rates (R_1) are in Mrad/s. Exposure (Φ) is calculated from NiEDDA data only. Specific activities (SA) are in percent of wild type hGIIA. Relaxation rates in the presence and in the absence of membrane *without relaxant* are between 0.25 and 0.6 Mrad/s.

hGIIA mutant	R_1 with 10 mM Crox			R_1 with 10 mM NiEDDA		Φ[c]	SA
	−DTPM[a]	+DTPM LUV[b]	+DTPM/Triton X-100 micelles[a]	−DTPM[a]	+DTPM/Triton X-100 micelles[b]		
							%
V3C-sl	>6	0.285	1.06	2.76	<0.58	0	82.5
K10C-sl	>5	0.270	1.13	3.5	0.467	6	100
L19C-sl	>11	0.231	0.81	6.7	0.309	0	102
F23C-sl	>5	0.261	0.50	3.7	0.285	0	85
S35C-sl	>10	—[d]	>10	5.4	5.4[e]	100	80
K56C-sl	>5	0.441	>10	3.7	3.7[e]	100	98.5
F63C-sl	>7	0.290	0.70	5.1	0.361	1	80
N70C-sl	>8	0.31	2.4	3.02	1.26	31	84.5
T104C-sl	>10	0.27	1.83	2.7	2.7[e]	100	105
S113C-sl	3.4	0.314	1.4	1.95	1.95[e]	100	90
K115C-sl	>6	0.286	1.04	3.01	0.383	5	63
S120C-sl	>10	0.541	>10	5.4	5.4[e]	100	100

[a] |Error| is ≤0.1 Mrad/s.
[b] |Error| is ≤0.01 Mrad/s.
[c] |Error| ≤2%, $\Phi = \Delta R_1^{bound}/\Delta R_1^{unbound}$.
[d] R_1 not measured for this condition.
[e] Need two rates (see text).

In the current study, we have introduced the use of the TD techniques SR and pELDOR to directly measure the shift ($\Delta R_1 = R_1^{+Relaxant} - R_1^{-Relaxant}$) in spin-lattice relaxation rate R_1 (Equation 3 in Ref. 14), as an alternative to the CW ΔP_2 measurement (14, 15). ΔR_1, like ΔP_2, is proportional to the local concentration of relaxant; however, the ΔR_1 measurement is often more accurate.[3] Both TD and CW data were acquired for hGIIA mutants in the presence and absence of DTPM LUV. Accurate measurement of the P_2 parameter in the presence of 10 mM Crox without membrane was impossible, due to a large electrostatic interaction between hGIIA and Crox (Fig. 1). ΔR_1 could only be obtained for one mutant (S113C-sl) in the absence of membrane (Table I). The protein-Crox interaction will be described below in detail. Fig. 1 shows typical CW data for spin-labeled hGIIA (S120C-sl), consisting of the four CW power saturation curves that define P_2 values in the presence and absence of membranes and Crox. The curve for protein without membranes and in the presence of Crox does not "roll over," indicating an inability to saturate the collisional relaxation process with experimentally realizable microwave powers. Decreasing the Crox concentration could bring this rollover into a detectable range, but would compress the resolution of Crox responsiveness for protein bound to membranes.

The response of membrane-bound S120C-sl to Crox measured by CW EPR (Fig. 1) is typical of data obtained for all 12 mutants on vesicles and represents a high degree of protection from Crox due to protein-membrane binding. The TD method confirms the CW results (Fig. 2, *upper left*, *±Crox*, *+DTPM*). The R_1 value without Crox, in the presence of membrane, for S120C-sl is 0.422 ± 0.007 Mrad/s; with Crox the R_1 value is 0.541 ± 0.007 Mrad/s (see Table I, column 2, +DTPM/LUV for conditions that include Crox). The value of R_1 in the presence of Crox, without membrane, is greater than 10 Mrad/s (Table I, column 1). Mutants V3C-sl, K10C-sl, and F23C-sl, which contain spin labels in the vicinity of the putative IBS, exhibited total protection from Crox by membranes. The small Crox-induced shift of S120C-sl is surprising, because this mutant is located on the face of the protein opposite the putative IBS, and a large exposure would be expected, as seen in previous applications of this EPR method (14, 15). The neutral relaxing agent

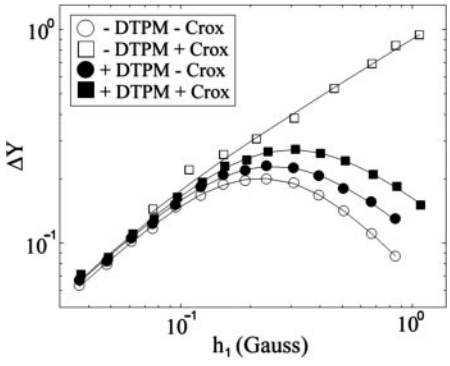

FIG. 1. **CW power saturation curves for mutant S120C-sl ± DTPM vesicles and ± 10 mM Crox.** h_1 is microwave power amplitude in Gauss, ΔY is the peak-to-peak height of the center field feature of the EPR spectrum (arbitrary units). Low power ΔY values for each of the conditions were rescaled to a common value. *Solid lines* are the fit to Equation 1 of Ref. 14.

NiEDDA was used to investigate S120C-sl on vesicles, because NiEDDA concentration is not modulated by the electrostatic potential of the anionic membrane or protein surface charge. A small R_1 shift of the same magnitude as that found with 10 mM Crox was measured for membrane bound hGIIA in the presence of 10 mM NiEDDA, reinforcing the conclusion of minimal exposure for S120C-sl to the aqueous phase (data not shown). The nearly uniform protection of all spin labels (Table I, columns 1 and 2) is qualitatively supported by the additional observation that the CW spectra of all mutants exhibit motional slowing of the spin label upon binding to membranes, suggesting a binding-induced steric interaction. Because the spin-labeled sites decorate multiple sectors of the protein surface, protection of all sites from Crox and NiEDDA implies limited accessibility of the entire surface of the membrane-bound protein to the aqueous phase.

To assess the depth of penetration of residues into the membrane hydrophobic core, ΔP_2 and ΔR_1 were measured in the presence and absence of O_2, which is an electrically neutral spin relaxant with a 4-fold higher concentration in the membrane hydrophobic core than in buffer (15, 18). No enhancement of O_2 relaxation was detected when protein was absorbed onto membranes, indicating that the spin-labeled residues did not access the O_2 in the membrane.[3]

[3] R. Nielsen, S. Canaan, J. G. Gladden, M. H. Gelb, and B. H. Robinson, manuscript in preparation.

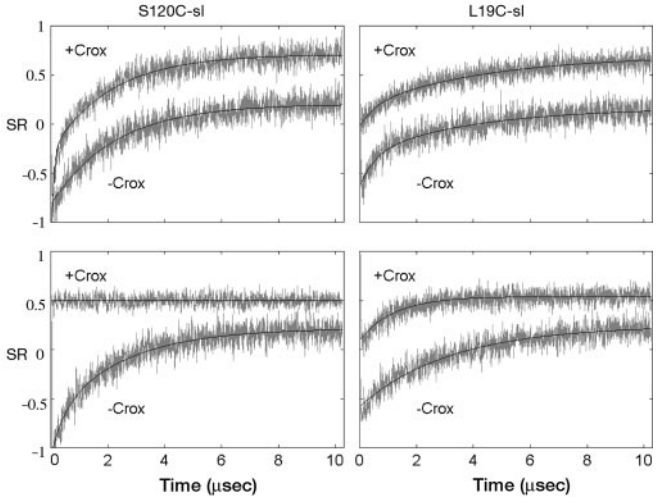

FIG. 2. **SR on the middle feature of the EPR manifold for S120C-sl (*left*) and L19C-sl (*right*) on vesicles (*top panels*) and mixed micelles (*bottom panels*), ±10 mM Crox.** Data used to obtain rates in Table I consisted of longer time acquisitions with typically four times more averaging than shown here.

Electrostatics of hGIIA—The large relaxivity of Crox for spin labels of hGIIA in the absence of membranes (Fig. 1, *open squares*; Table I, column 1) would appear to be due to an attraction of anionic Crox (nominal charge −3) to the highly cationic surface of hGIIA (pI = 9.39). This implies a greater influence of protein electrostatic interactions than seen in our previous EPR studies (14, 15). We quantified this interaction to understand the possible role of protein electrostatics in binding of hGIIA to anionic vesicles. The electrostatic potential of hGIIA was investigated at three sites (S35C-sl, N70C-sl, and S120C-sl). The universally strong ΔP_2 or ΔR_1 response to Crox found in the absence of membrane provides a means of site specifically probing the protein electrostatic potential. Line broadening of the CW spectrum at site S35C-sl as a function of Crox concentration (0.05–10 mM) indicated a local concentration of Crox that exceeds the bulk concentration by at least a factor of 10. For example, ~4.5 Gauss of line width broadening was observed for S35C-sl with 10 mM Crox instead of the ~0.5 Gauss expected for a spin-labeled neutral protein under the same electrolyte conditions (14, 15).[3] This enhancement of Crox relaxivity implies a local positive protein surface potential (Ψ) on the order of + 25 mV, if a simple electrostatic Boltzmann distribution is assumed, using the z = −3 nominal charge of Crox.

$$\left(\frac{[\text{Crox}]}{[\text{Crox}]_o} \approx \frac{4.5}{0.5} = e^{-z\Psi/k_BT}\right) \qquad \text{(Eq. 1)}$$

The potential at site N70C-sl was probed by CW and TD measurements of the relaxivity of 0.5 mM Crox as a function of NaCl concentration (0–300 mM). The ΔP_2 shift was weighted by the linewidth for comparison with ΔR_1 (18). These results show a strong non-linear attenuation of Crox relaxation with increasing salt concentration. The data will be published elsewhere.[3] The electrostatic screening due to salt was modeled using Gouy-Chapman theory with a +25 mV value of the protein electrostatic potential (29).[3] Response to neutral NiEDDA was measured under similar salt conditions and showed no dependence on NaCl concentration, as expected. The potential at site S120C-sl was measured with a TD technique that uses the ΔR_1 response to positive (TEMPAMINE), negative (CTPO), and neutral (TEMPOL) ^{15}N nitroxides and yielded a protein-surface potential of +(21 ± 3) mV (14, 24, 25).[3] In light of the strong relaxation of nitroxides by Crox found for all of the mutants, these measurements may be taken as indicative of the overall positive potential that the protein presents. This conclusion is supported by the nearly uniform distribution of the 23 cationic surface residues over the entire protein surface (30).

To further test the dependence of the protein electrostatics on local environment, we used a mutant in which four cationic charges close to and surrounding the spin label were charge reversed (E56C-sl/K52E/R53E/K56E/R57E). As a control, we studied (S120C-sl/K52E/R53E/K56E/R57E) in which the spin label is 21 Å from the closest charge reversal site. It was possible to obtain a P_2 value typical of a neutral protein site for the former mutant. In the latter case the P_2 value remained unmeasurable when 10 mM Crox was added, because the strong electrostatic interaction was locally retained. These results, like the studies described above, show that the strong relaxation of spin label by Crox in the absence of membranes is due to the highly cationic nature of the surface of hGIIA.

Light Scattering Studies—Several hypotheses were considered to account for the nearly complete lack of aqueous phase exposure to Crox of all of the spin labels on hGIIA in the presence of anionic membranes. Penetration of the protein into the aqueous lumen of the LUV seems unlikely and was ruled out by the observation that membrane-dependant protection of S120C-sl from Crox was the same regardless of whether LUV did or did not contain lumenal Crox. It also seems unlikely that the LUV bilayer could achieve a sufficiently high degree of curvature to wrap around hGIIA (diameter ~40 Å) or to internalize it via an endocytic-type mechanism. Right angle light scattering of vesicles alone increased by 150% when hGIIA was added to a solution of DTPM LUV in EPR buffer (protein/lipid ratio was the same as for the EPR samples). Using a particle analyzer, DTPM LUV without hGIIA were found to have a mean diameter of 101 nm and a distribution width at half-peak of 30 nm. In contrast, the mean particle diameter was 1150 nm for samples containing DTPM LUV and hGIIA. The size distribution was bimodal with repartitions falling in the ranges 65–112 nm and 968–1986 nm, indicating the formation of vesicle clusters in the presence of hGIIA. No increase in light scattering or particle size was seen when bee venom sPLA$_2$ (pI = 7.8) or human group X sPLA$_2$ (pI = 5.1) was added to DTPM LUV, indicating that the binding of these proteins to the vesicles did not induce aggregation. The large increase in scattering seen with hGIIA rules out endocytic-type and wrapping mechanisms and demonstrates that a supramolecular structure involving multiple LUV is formed.

Light scattering was also carried out with zwitterionic $DO_{et}PC$ vesicles containing various amounts of anionic $DO_{et}PS$. A minimum value between 20 and 30% $DO_{et}PS$ was found to be necessary for protein binding with EPR buffer conditions and was accompanied by a 180% increase in light scattering.

TD EPR Data from Spin-labeled hGIIA on DTPM/Triton X-100 Mixed Micelles—We also carried out EPR studies using spin-labeled hGIIA proteins bound to micelles of Triton X-100 containing 10 mole percent DTPM (mixed micelles). Dennis and co-workers (31) have shown that sPLA$_2$s display high enzymatic activity on mixed micelles, although substrate replenishment in enzyme containing mixed micelles may limit the catalytic turnover (1). It was found that the spin label S120C-sl, located on the face opposite the IBS, was exposed to Crox and NiEDDA when protein was bound to mixed micelles. The EPR data were more in line with our previous membrane docking studies in which spin labels can be differentiated by their proximity to the lipid interface (14, 15).

With hGIIA bound to mixed micelles, a full range of exposure

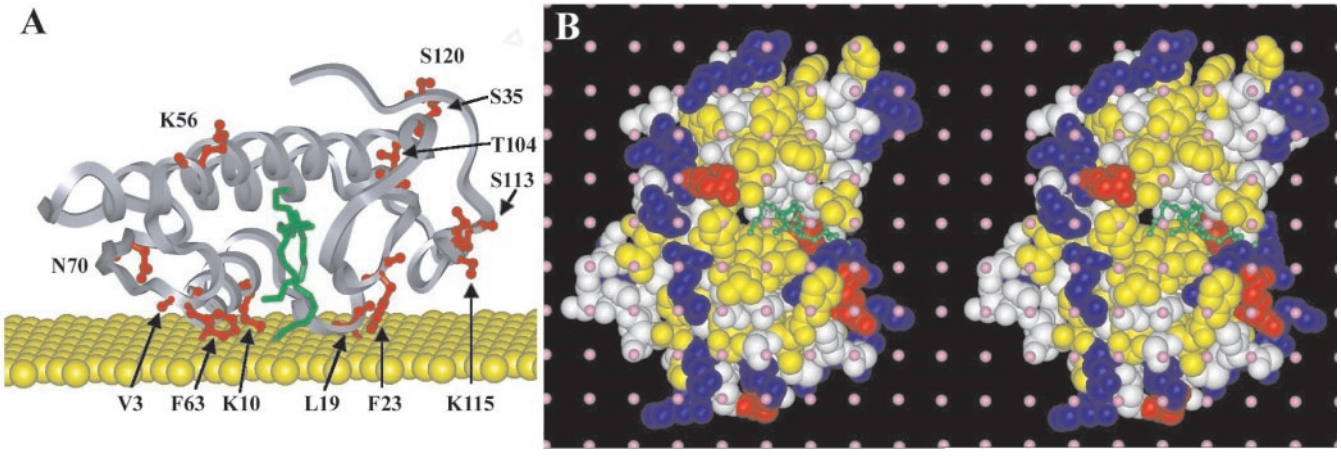

FIG. 3. *A*, orientation of hGIIA on mixed micelles using NiEDDA exposure data. The phospholipid analog bound to hGIIA, as seen in the x-ray structure (26), is in *green*. Spin label sites are *red*. The membrane surface is represented as *yellow balls* (radius is 2.5 Å). *B*, stereoview of docked hGIIA as viewed perpendicular to the membrane interface (*pink balls*): Lys and Arg (*blue*), Glu and Asp (*red*), hydrophobics (Ala, Val, Leu, Ileu, Trp, Phe, Met, Tyr) (*yellow*), and inhibitor is *green*.

to Crox and NiEDDA were found for the complete set of spin-labeled mutants. Table I presents the R_1 values in the presence and absence of micellar interface for 10 mM Crox or NiEDDA. R_1 values in the absence of relaxing agent were found to be between 0.25 and 0.6 Mrad/s for protein both in the presence or absence of mixed micelles. The first column of Table I contains lower bounds for the Crox rates without membrane, when the value was unmeasurable. These lower bounds in most cases represent early time base-line artifacts that could not be rigorously distinguished from a real signal arising from electrostatically enhanced relaxivity of Crox (see above). The third column is the R_1 rate in the presence of mixed micelles and 10 mM Crox. Mutants, containing spin labels that are fully exposed to the aqueous solution (S35C-sl, K56C-sl, S120C-sl), exhibit the same large relaxation as found in the absence of mixed micelles. Most of the remaining sites have ΔR_1^{bound} values that are small in comparison with the values of $\Delta R_1^{unbound}$ (without mixed micelles). Therefore, the spin labels of the membrane-bound protein appear to be protected from Crox. An exception is found in the case of S113C-sl, whose value of $\Delta R_1^{bound}/\Delta R_1^{unbound}$ represents about 30% exposure.

Fig. 2 shows TD saturation recovery (from which R_1 is obtained) for S120C-sl and L19C-sl, both on LUV and mixed micelles in the presence and absence of 10 mM Crox. L19C-sl is protected both on LUV and mixed micelles (*right side*), and S120C-sl is protected on LUV (*left side, top*), but exposed on mixed micelles (*left side, bottom*). Large R_1 values appear as faster decays in the SR spectrum. The rate for S120C-sl when it is bound to mixed micelles in the presence of Crox is so fast that it shows up as a *flat line* (*lower left*). NiEDDA was used to discern which of the residues protected from Crox were also protected from the neutral relaxant. For example, T104C-sl and N70C-sl show similar R_1^{bound} values in the presence of Crox, but are distinguished in the case of NiEDDA exposure (Table I). Those proteins exhibiting a full exposure to NiEDDA (footnoted *e* in Table I) also produced a second minor component consistent with partial protection. The SR spectrum for such fast rates, resulting from fully exposed enzyme, is very sensitive to any slower relaxing minor binding component. The second slower rate, whose amplitude did not exceed 20% of the fast rate, was necessary to account for this baseline. As in the case of hGIIA bound to LUV, O_2 exposure data with DTPM/Triton X-100 mixed micelles showed no enhancement relative to the protein in the absence of lipid aggregate.[3] This is consistent with a minimal penetration of the nitroxides into the hydrophobic environment of the lipid.

Docking hGIIA at the Surface of Mixed Micelles—To dock hGIIA at the surface of DTPM/Triton X-100 mixed micelles, we assumed that the conformation seen in the x-ray structure (26) does not change significantly upon interfacial binding. The orientation of hGIIA on the interface was obtained by insisting that residues, which showed no Crox or NiEDDA exposures, are located at the protein-micelle interface, with minimal penetration as suggested by O_2 data. Protected residues (Val^3, Lys^{10}, Leu^{19}, Phe^{23}, and Phe^{63}) were fit to a common plane that was parameterized by two angles and a translation. Two orientations were found to be optimal and are related by 14° rotation about a hinge, consisting of Lys^{10} and Phe^{63}, that spans a distance of 25 Å parallel to the membrane surface. Only one of these orientations (Fig. 3A) was consistent with the intermediate exposure found for sites S113C-sl and N70C-sl, the other orientation brought residue S113C-sl too close to the membrane and N70C-sl farther from the membrane, in contradiction to the Crox and NiEDDA data.

Fig. 3*B* shows the different residues involved in the IBS. The IBS is composed mainly of six hydrophobic residues (Val^3, Ala^{18}, Leu^{19}, Phe^{23}, Phe^{63}, and Tyr^{111}), two basic residues (Arg^7 and Lys^{10}), a single acidic residue (Glu^{16}), and a single neutral residue (His^6), all in contact with the interface. In addition, there are two other basic residues (Lys^{67} and Lys^{107}) that lie 4–5 Å from the membrane surface.

DISCUSSION

The TD EPR techniques allowed us to dock hGIIA at the surface of mixed micelles despite the strong influence of protein electrostatics on Crox concentration. The TD and CW EPR results showing protection by anionic DTPM LUV for numerous spin labels scattered over the entire surface of hGIIA were unexpected. The increase in scattering expected if hGIIA brings only two vesicles in close proximity is negligible compare with the 150% increase observed. The light scattering data indicate the formation of vesicle clusters with >100 participants. The EPR data, showing complete protection for all spin-labeled sites, is consistent with this conclusion. The EPR data rules out a simple model wherein two vesicles are bridged through a few enzymes such that the IBS is bound to one vesicle, and the opposite face of the protein is bound to a second vesicle, because there would be a significant amount of protein still exposed. We are left with the suggestion that hGIIA segregates into islands on vesicles such that patches of protein are sandwiched between vesicles and protected from solution phase relaxants. Having ruled out both the possibility that the

proteins are encapsulated by membrane and a mechanism in which only two vesicles are bridged together by enzyme, we are forced to consider a model involving a supramolecular structure. In the simplest of such models, we assume that all proteins gather into patches that form the connection points between LUV, with the latter assembled into a simple cubic lattice arrangement. Since there are ~150 proteins per LUV, there would be ~50 hGIIA proteins per patch. One might imagine that within the patch the proteins are in molecular contact with each other. In this model only those proteins that are on the peripheral edge of the patch can be accessed by Crox. A better packing model is to assume that the proteins are about 45 Å apart, as compared with the protein diameter of 36 Å, since this would generate a nearly electrically neutral patch. An electrostatic calculation (see "Materials and Methods") shows that the repulsion between the LUV is more that offset by the attraction for the patch of protein. In this arrangement although there is room in the inter-protein spaces for Crox molecules, the presence of two strongly negative charged membrane surfaces (about 40 Å apart) would be expected to repel Crox molecules.

Further studies showed that addition of 200 mM NaCl largely prevented the increase in light scattering that occurred when hGIIA was added to 30% DO$_{et}$PS, 70% DO$_{et}$PC LUV. Under these conditions, EPR data indicated that the spin label on the face of the protein opposite the IBS, S120C-sl, showed increased mobility and a larger exposure to Crox, but retained features of both protected and unprotected populations (data not shown). Apparently the addition of salt only partially suppresses the formation of the protein-vesicle supramolecular aggregate at the relatively high protein and LUV concentrations in the EPR sample compared with the samples analyzed by light scattering. On the other hand, the nitroxide of V3C-sl continued to show complete protection from Crox and did not undergo a mobility change upon addition of salt. These results are consistent with an electrostatic mechanism for hGIIA-induced LUV aggregation, yet the binding of hGIIA via its IBS to the membrane surface is maintained in the presence of NaCl. The latter result suggests that the numerous IBS hydrophobic residues (Fig. 3) play a substantial role in anchoring the protein to the surface of LUV.

hGIIA bound to mixed micelles of detergent and anionic phospholipid should be mono-disperse. This is because the mixed micelle (diameter ~100 Å (32)) is only slightly larger than hGIIA, and thus it is not possible to form an island of several enzymes bound to the same mixed micelle. The EPR data (Table I) show, in fact, that only the face of hGIIA that includes the opening to the active site slot is protected from Crox and NiEDDA in the presence of DTPM/Triton X-100 mixed micelles and that this face constitutes the IBS. When the amount of DTPM in Triton X-100 mixed micelles was increased to 20 mol % or higher, S120C-sl, which is on the face of the enzyme opposite the IBS, becomes protected from Crox. This suggests that a lamellar phase (*i.e.* vesicles) is forming when the DTPM/Triton X-100 ratio is increased, as expected since mixed micelles form only when the mole ratio of detergent to phospholipid exceeds about 3 (1, 32).

The supramolecular aggregation model not only explains the strict dependence of the interfacial binding of hGIIA on a critical mole fraction of anionic phospholipid in the zwitterionic interface, but it also explains a number of unusual observations reported for hGIIA. Several sPLA$_2$s bind sufficiently tightly to anionic phosphatidylmethanol vesicles and hydrolyze the outer layer phospholipids in a processive manner, *i.e.* without desorption of enzyme into the aqueous phase (termed scooting (33)). In contrast, hGIIA was found to hydrolyze phosphatidylmethanol vesicles in a partially scooting manner in which the enzyme slowly hops between vesicles (34). Given the highly cationic surface of hGIIA, this result was surprising. In light of the current study, it is tempting to suggest that hGIIA, in segregated patches between two vesicles, can "roll over" such that its IBS, bound to one vesicle, comes in contact with a nearby vesicle in the complex.

Recent studies have been carried out in which binding of hGIIA to vesicles is quantified by measuring the amount of enzyme remaining in the supernatant when sucrose-loaded vesicles are pelleted by centrifugation. These studies show that hGIIA does not bind to DO$_{et}$PC vesicles, but that binding increases dramatically when the amount of anionic phospholipid DO$_{et}$PS is increased from 20–30 mol %.[2] Based on the EPR and light scattering studies reported here, it can now be said that interfacial binding of hGIIA is not a simple process involving the formation of a mono-disperse enzyme-vesicle complex. Thus, quantification of interfacial binding of hGIIA to anionic vesicles by assigning a simple dissociation equilibrium constant, K_d, for the desorption of enzyme from the vesicle surface to the aqueous phase, as has been done previously (30), is inappropriate; the observed K_d must now be considered an apparent equilibrium constant. Other, less basic enzymes, including pig pancreatic (35), bee venom, and human group X sPLA$_2$s (see "Results"), do not cause vesicle aggregation, and interfacial binding in these cases can be described by a simple K_d value. We have recently found that mutation of IBS cationic residues Arg^7 and Lys^{10} of hGIIA to glutamates (charge reversal) results in only a modest, ~10-fold reduction in interfacial binding to DO$_{et}$PS/DO$_{et}$PC vesicles.[2] This result was surprising because these cationic residues lie on the IBS (Fig. 3). Their modest contribution to interfacial binding can now be explained by the current study considering the likely possibility that many of the 23 surface lysine and arginine residues contribute to the formation of the protein-lipid aggregate, and thus mutating only two of them results in a modest reduction in binding. Additionally, we have found that charge reversal mutation of four basic residues on the face of hGIIA opposite the IBS (K52E/R53E/K56E/R57E) also leads to a ~10-fold reduction in binding to DO$_{et}$PS/DO$_{et}$PC vesicles.[2] The model developed wherein several hGIIA basic residues scattered over multiple faces of the protein contribute to supramolecular aggregate formation provides an explanation of all of the charge reversal mutagenesis data.

Our docking of hGIIA on mixed micelles may be compared with recent prediction for porcine pancreatic IB sPLA$_2$. The x-ray structure of this enzyme, which is structurally homologous to hGIIA, has been obtained in the presence of an active site-directed inhibitor and a high concentration of phosphate (or sulfate) (36). In this structure, the polar headgroup of the inhibitor is bound to the active site of one sPLA$_2$, and the long hexadecyl chain of this inhibitor interacts with the active site of an opposing sPLA$_2$ molecule. Hydrophobic residues on the putative IBS of both proteins are in van der Waals contact with each other, and five phosphate anions that are approximately co-planar are seen at the perimeter of this hydrophobic contact patch. It has been suggested that this plane defined by the phosphates mimics the planar array of phospholipid phosphates of a membrane surface. The orientation of the membrane plane determined by the EPR method for hGIIA (Fig. 3) differs from the orientation proposed for the pancreatic sPLA$_2$. If hGIIA is bound to the membrane as proposed for the pancreatic enzyme, Ser^{113} should be against the membrane yet this residue shows Crox and NiEDDA exposure (Table I). Additionally, the proposed IBS for pancreatic sPLA$_2$ would leave Lys^{10} partially exposed to the aqueous phase and leave Asn^{70} and

Thr^{104} fully exposed, yet the EPR data clearly show a different pattern of Crox and NiEDDA exposures. The IBS depicted in Fig. 3 leaves the long axis of the active site slot nearly perpendicular to the membrane plane as opposed to the near parallel orientation suggested for pancreatic sPLA$_2$.

REFERENCES

1. Berg, O. G., Gelb, M. H., Tsai, M. D., and Jain, M. K. (2001) *Chem. Rev.* **101,** 2613–2654
2. Han, S. K., Kim, K. P., Koduri, R., Bittova, L., Munoz, N. M., Leff, A. R., Wilton, D. C., Gelb, M. H., and Cho, W. (1999) *J. Biol. Chem.* **274,** 11881–11888
3. Han, S. K., Yoon, E. T., Scott, D. L., Sigler, P. B., and Cho, W. (1997) *J. Biol. Chem.* **272,** 3573–3582
4. Gadd, M. E., and Biltonen, R. L. (2000) *Biochemistry* **39,** 9623–9631
5. Gelb, M. H., Cho, W., and Wilton, D. C. (1999) *Curr. Opin. Struct. Biol.* **9,** 428–432
6. Bezzine, S., Koduri, R. S., Valentin, E., Murakami, M., Kudo, I., Ghomashchi, F., Sadilek, M., Lambeau, G., and Gelb, M. H. (2000) *J. Biol. Chem.* **275,** 3179–3191
7. Buckland, A. G., and Wilton, D. C. (2000) *Biochim. Biophys. Acta* **1488,** 71–82
8. Foreman-Wykert, A. K., Weiss, J., and Elsbach, P. (2000) *Infect. Immun.* **68,** 1259–1264
9. Koduri, R. S., Gronroos, J. O., Laine, V. J., Le Calvez, C., Lambeau, G., Nevalainen, T. J., and Gelb, M. H. (2002) *J. Biol. Chem.* **277,** 5849–5857
10. Beers, S. A., Buckland, A. G., Koduri, R. S., Cho, W., Gelb, M. H., and Wilton, D. C. (2002) *J. Biol. Chem.* **277,** 1788–1793
11. Qu, X. D., and Lehrer, R. I. (1998) *Infect. Immun.* **66,** 2791–2797
12. Koduri, R. S., Baker, S. F., Snitko, Y., Han, S. K., Cho, W., Wilton, D. C., and Gelb, M. H. (1998) *J. Biol. Chem.* **273,** 32142–32153
13. Murakami, M., Koduri, R. S., Enomoto, A., Shimbara, S., Seki, M., Yoshihara, K., Singer, A., Valentin, E., Ghomashchi, F., Lambeau, G., Gelb, M. H., and Kudo, I. (2001) *J. Biol. Chem.* **276,** 10083–10096
14. Lin, Y., Nielsen, R., Murray, D., Hubbell, W. L., Mailer, C., Robinson, B. H., and Gelb, M. H. (1998) *Science* **279,** 1925–1929
15. Ball, A., Nielsen, R., Gelb, M. H., and Robinson, B. H. (1999) *Proc. Natl. Acad. Sci. U. S. A.* **96,** 6637–6642
16. Dudler, T., Chen, W. Q., Wang, S., Schneider, T., Annand, R. R., Dempcy, R. O., Crameri, R., Gmachl, M., Suter, M., and Gelb, M. H. (1992) *Biochim. Biophys. Acta* **1165,** 201–210
17. Jain, M. K., and Gelb, M. H. (1991) *Methods Enzymol.* **197,** 112–125
18. Altenbach, C., Greenhalgh, D. A., Khorana, H. G., and Hubbell, W. L. (1994) *Proc. Natl. Acad. Sci. U. S. A.* **91,** 1667–1671
19. Yager, T. D., Eaton, G. R., and Eaton, S. S. (1979) *Inorg. Chem.* **18,** 725–727
20. Hixon, M. S., Ball, A., and Gelb, M. H. (1998) *Biochemistry* **37,** 8516–8526
21. Mailer, C., Haas, D. A., Hustedt, E. J., Gladden, J. G., and Robinson, B. H. (1991) *J. Magn. Reson.* **91,** 475–496
22. Mailer, C., Danielson, J. D. S., and Robinson, B. H. (1985) *Rev. Sci. Instrum.* **56,** 1917–1925
23. Robinson, B. H., Haas, D. A., and Mailer, C. (1994) *Science* **263,** 490–493
24. Yin, J.-J., and Hyde, J. S. (1987) *J. Magn. Reson.* **74,** 82–93
25. Shin, Y. K., and Hubbell, W. L. (1992) *Biophys. J.* **61,** 1443–1453
26. Scott, D. L., White, S. P., Browning, J. L., Rosa, J. J., Gelb, M. H., and Sigler, P. B. (1991) *Science* **254,** 1007–1010
27. Stahelin, R. V., and Cho, W. (2001) *Biochemistry* **40,** 4672–4678
28. Mounier, C. M., Luchetta, P., Lecut, C., Koduri, R. S., Faure, G., Lambeau, G., Valentin, E., Singer, A., Ghomashchi, F., Beguin, S., Gelb, M. H., and Bon, C. (2000) *Eur. J. Biochem.* **267,** 4960–4969
29. Lakshminarayanaiah, N. (1984) *Equations of Membrane Biophysics*, Academic Press, New York
30. Snitko, Y., Koduri, R. S., Han, S. K., Othman, R., Baker, S. F., Molini, B. J., Wilton, D. C., Gelb, M. H., and Cho, W. (1997) *Biochemistry* **36,** 14325–14333
31. Carman, G. M., Deems, R. A., and Dennis, E. A. (1995) *J. Biol. Chem.* **270,** 18711–18714
32. Robson, R. J., and Dennis, E. A. (1983) *Acc. Chem. Res.* **16,** 251–258
33. Jain, M. K., Ranadive, G., Yu, B. Z., and Verheij, H. M. (1991) *Biochemistry* **30,** 7330–7340
34. Bayburt, T., Yu, B. Z., Lin, H. K., Browning, J., Jain, M. K., and Gelb, M. H. (1993) *Biochemistry* **32,** 573–582
35. Jain, M. K., Egmond, M. R., Verheij, H. M., Apitz-Castro, R., Dijkman, R., and De Haas, G. H. (1982) *Biochim. Biophys. Acta* **688,** 341–348
36. Pan, Y. H., Epstein, T. M., Jain, M. K., and Bahnson, B. J. (2001) *Biochemistry* **40,** 609–617